Commun Nonlinear Sci Numer Simulat 127 (2023) 107582

Contents lists available at ScienceDirect

Communications in Nonlinear Science and Numerical Simulation

journal homepage: www.elsevier.com/locate/cnsns

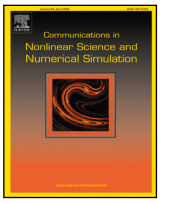

Research paper

Rough volatility via the Lamperti transform

Sergio Bianchi [a,*], Daniele Angelini [a], Augusto Pianese [b], Massimiliano Frezza [a]

[a] MEMOTEF, Sapienza University of Rome, Italy
[b] Quantlab, University of Cassino and Southern Lazio, Italy

ARTICLE INFO

Keywords:
Rough volatility
Fractional Ornstein–Uhlenbeck process
Self-similarity
Hurst–Hölder exponent

ABSTRACT

We study the roughness of the log-volatility process by testing the self-similarity of the process obtained by the de-Lampertized realized volatility. The value added of our analysis rests on the application of a distribution-based estimator providing results which are more robust with respect to those deduced by the scaling of the individual moments of the process. Our findings confirm the roughness of the log-volatility process.

1. Introduction

Rough volatility models incorporate the idea that volatility exhibits complex patterns like high frequency fluctuations, clustering and heavy tails, revealed by trajectories that are less Hölder continuous than those of Brownian motion. The growing interest in this field has motivated several variants of standard models: the Rough Fractional Stochastic Volatility model [1], the Rough Bergomi model [2] or the Rough Heston model [3], just to mention the main formulations.

Many contributions have focused on estimation and found evidence consistent with the roughness of volatility as initially described in the work of Gatheral et al. [1], where the authors point out that the logarithm of realized variance behaves essentially as a fractional Brownian motion (fBm) with Hurst exponent H of order 0.1. Using the generalized Hurst exponent, Livieri et al. [4] analyze the spot volatility approximations given by implied volatilities of at-the-money options on the S&P500 index and find a level of roughness moderately higher ($H \simeq 0.3$) than that estimated by previous contributions (the authors explain this result by the smoothing effect due to the remaining time to maturity of the considered options).

Motivated by simulations suggesting the presence of an estimation error of latent volatility which can result in an illusive scaling property with a rough parameter, Fukasawa et al. [5] develops a quasi-likelihood estimator and concludes that the volatility is even rougher than what estimated in previous literature. Exploiting the GMM framework, similar findings ($H \lesssim 0.05$) are obtained by Bolko et al. [6] for a large panel of equity indices. To explain these close to zero values of H, Peng et al. [7] introduce a family of random measures to consider within the same framework multifractal and rough volatility models. Bennedsen et al. [8] confirm roughness for the log-volatility of thousands of stocks by performing OLS estimates based on the second order variogram. Using the multifractal detrended fluctuation analysis, Takaishi [9] finds roughness in Bitcoin volatility and non costant generalized Hurst exponent, signature of a multifractality partly ascribable to the distributional properties of log-volatility. From a modeling perspective, Fukasawa [10] proves that non-rough volatility models are inconsistent with a short-time power law of volatility skew and that, given a short-time power law of volatility skew in an option market, a continuous price dynamics of the underlying asset with non-rough volatility admits an arbitrage. Brandi and Di Matteo [11] analyze the interplay between price multiscaling and volatility roughness and find that, although the rough Bergomi model with a low value of the Hurst exponent can reproduce multiscaling features of the prices' time series, it fails to reproduce the negative dependency between prices' multiscaling and the Hurst exponent of the volatility process. Recent contributions have questioned the above results and suggested that the apparent

* Corresponding author.
E-mail address: sergio.bianchi@uniroma1.it (S. Bianchi).

https://doi.org/10.1016/j.cnsns.2023.107582
Received 3 July 2023; Received in revised form 24 September 2023; Accepted 27 September 2023
Available online 30 September 2023

roughness observed in realized volatility can be ascribed to microstructure noise rather than the volatility process itself. On this line is the paper by Cont and Das [12], who use a non-parametric method based on normalized pth variation along a sequence of partitions and show numerically that, even when the instantaneous volatility has diffusive dynamics with the same roughness as Brownian motion, the realized volatility exhibits rough behavior corresponding to a Hurst exponent significantly smaller than 0.5. Rogers [13] suggests that the roughness of volatility can be explained also by simpler models such as a bivariate Ornstein–Uhlenbeck model. Angelini and Bianchi [14] consider a Fractional Stochastic Regularity Model and provide some evidence of potential highly nonlinear biases when the Hurst exponent is estimated by smoothing moment-based methodologies.

In order to address the potential ambiguity associated with moment-based estimators, we assess the irregularity of log-volatility directly through the analysis of how its realized probability distribution scales, as opposed to relying solely on its individual statistical moments. We exploit the Lamperti transform to convert the realized log-volatility into a self-similar sequence X_t. Then we study the self-similarity parameter of this sequence by the non parametric and distribution-based estimator introduced by Bianchi [15]. Roughly speaking, the estimator can be defined as the diameter of the space generated by the rescaled distribution functions of X_t and it is calculated as the value which minimizes the maximal pairwise distance of the elements of this space. Being based on the whole distributions, the estimates are more robust and can be evaluated not only by visual inspection but in terms of their statistical significance. In fact, in the one-dimensional case, the diameter reduces to the Kolmogorov–Smirnov statistic, thus allowing to apply a test to evaluate the statistical significance of the estimated self-similarity parameter. Applied to real financial data, the method confirms the roughness of log-volatility for 21 out of 21 considered stock indices, with values of the Hurst exponent ranging from 0.060 to 0.151.

The remainder of the paper is organized as follows. In Section 2 we recall the definition of self-similarity, the Lamperti transform and introduce the diameter of the space of rescaled distributions along with its main properties. In Section 4 we show that the Lamperti transform of the Ornstein–Uhlenbeck process driven by a fBm of parameter H_0 is self-similar with parameter H_0, regardless the value of H used in the transform. Section 5 is devoted to the empirical application. Finally, Section 6 concludes.

2. Self-similar stochastic processes

In this Section we will recall some definitions and theorems that will be used in Section 4 to justify the methodology that we propose to estimate the roughness of the log-volatility.

Definition 2.1 (*Lamperti [16]*). The $\mathbb{R}^k-$ valued stochastic process $\{X_t, t \geq 0\}$, nontrivial and stochastically continuous[1] at $t = 0$, is *self-similar* with parameter $H_0 \geq 0$ (H_0-ss) if for any $a > 0$,

$$\{X_{at}\} \overset{d}{=} \{a^{H_0} X_t\} \tag{1}$$

where $\overset{d}{=}$ denotes the equality of the finite-dimensional distributions of X_t.[2]

Remark 2.1. Since it can be proved that (a) $H = 0$ if and only if $X_t = X_0$ almost surely for every $t > 0$ and that (b) if $\mathbb{E}(|X_1|) < \infty$, then $H \leq 1$ [see [17]], to exclude degenerate cases in the following we will assume that $0 < H \leq 1$.

Remark 2.2. Observe that equality (1) implies $X_0 = 0$ a.s. Furthermore, from Definition 2.1 it readily follows that if X_t is self-similar and has stationary increments then increments are also self similar with the same parameter H_0 (H_0-sssi), that is:

$$\{X_{t+a} - X_t\} \overset{d}{=} \{a^{H_0}(X_{t+1} - X_t)\}. \tag{2}$$

In fact, being $X_0 = 0$ a.s., one has

$$\{X_{at}\} \overset{d}{=} \{a^{H_0} X_t\} \iff \{X_{at} - X_0\} \overset{d}{=} \{a^{H_0}(X_t - X_0)\}$$

For $t = 1$, it is

$$\{X_a - X_0\} \overset{d}{=} \{a^{H_0}(X_1 - X_0)\}$$

and this, by stationarity, implies (2).

If X_t was the log-price at time t, Eq. (2) would state that the a-lagged log-change distributes as a^{H_0} times the one-lag log-change, provided of course that the returns form a self-similar sequence. This scaling property has relevant implications, for example to assess dynamically the liquidity of the market [18].

[1] X_t is trivial if it is constant almost surely for every t and it is stochastically continuous at t if for any $\epsilon > 0$, $\lim_{h \to 0} \mathbf{P}\{|X_{t+h} - X_t| > \epsilon\} = 0$.

[2] The two stochastic processes $\{X_t : t \geq 0\}$ and $\{Y_t : t \geq 0\}$, defined on probability spaces $(\Omega, \mathcal{F}, \mathbf{P})$ and $(\tilde{\Omega}, \tilde{\mathcal{F}}, \tilde{\mathbf{P}})$ respectively and sharing the same state space $(R^k, \mathcal{B}(\mathbb{R}^k))$, are said to have the same finite dimensional distributions if, for any integer $n \geq 1$ and real numbers $0 \leq t_1 \leq t_2 \leq \cdots \leq t_n < \infty$ and $A \in \mathcal{B}(\mathbb{R}^k)$, it is:

$$\mathbf{P}((X_{t_1}, \ldots, X_{t_n}) \in A) = \tilde{\mathbf{P}}((Y_{t_1}, \ldots, Y_{t_n}) \in A).$$

A theorem which is pivotal for our purposes is the following generalization to self-similar processes of the Doob [19] transform:

Theorem 2.1 (*Lamperti [16]*). *If* $\{X_t, t \geq 0\}$ *is* H*-ss and*

$$V_t = e^{-tH} X_{e^t}, t \in \mathbb{R}, \tag{3}$$

then $\{V_t, t \in \mathbb{R}\}$ *is stationary.*

Conversely, if $\{V_t, t \in \mathbb{R}\}$ *is a stationary process and if for some* $H > 0$

$$X_t = t^H V_{\log t}, \text{ for } t > 0; \; X_0 = 0, \tag{4}$$

then $\{X_t, t \geq 0\}$ *is* H*-ss.*

When V_t is the log-volatility and follows a fractional Ornstein–Uhlenbeck process (which is stationary), Eq. (4) of Theorem 2.1 ensures that its Hurst exponent can be estimated as the self-similarity exponent of its Lamperti transform. This is the focus of our contribution: we exploit relation (4) to convert the log-volatility into a self-similar sequence, whose parameter we estimate by analyzing how its distributions scale over a set of timescales. The self-similarity parameter thus estimated coincides with the Hurst exponent of the log-volatility. Using the entire distribution for estimating the Hurst exponent appears more robust than using its individual moments, because these are typically estimated through methods that can potentially bias the results due to both the inherent variance of the estimators and the smoothing techniques often used.

Equality (1) [resp. (2)] can be tested through the Kolmogorov–Smirnov (KS) test applied to the diameter of the rescaled probability distribution functions (pdf) [15]. In order to use the KS test, we will restrict ourselves to the one-dimensional case ($k = 1$), although the theoretical results set forth apply for any k.

Given the compact set of timescales $\mathcal{A} = [\underline{a}, \overline{a}] \subset \mathbb{R}^+$, for any $a \in \mathcal{A}$, denote by $F_{X_{at}}(x)$ the cumulative distribution function of X_{at}. Eq. (1) can be written as[3]

$$F_{X_{at}}(x) := \mathbf{P}\left(X_{at} < x\right) = \mathbf{P}\left(a^{H_0} X_t < x\right) = F_{X_t}(a^{-H_0} x), \tag{5}$$

or, introducing the variable H, as

$$F_{a^{-H} X_{at}}(x) := \mathbf{P}\left(a^{-H} X_{at} < x\right) = \mathbf{P}\left(a^{H_0 - H} X_t < x\right) = F_{X_t}(a^{H - H_0} x). \tag{6}$$

Let us denote now by $\Psi_H := \{F_{a^{-H} X_{at}}(x), a \in \mathcal{A}, x \in \mathbb{R}\}$ the set of the distribution functions of $\{a^{-H} X_{at}\}$ and consider the distance function ρ induced by the sup-norm $\|\cdot\|_\infty$ with respect to $\mathcal{A}$. The diameter of the metric space $\left(\Psi_H, \rho\right)$ is then defined as

$$\begin{aligned} \delta_{X_t}(\Psi_H) &:= \sup_{x \in \mathbb{R}} \sup_{a,b \in \mathcal{A}} |F_{a^{-H} X_{at}}(x) - F_{b^{-H} X_{bt}}(x)| \\ &= \sup_{x \in \mathbb{R}} \sup_{a,b \in \mathcal{A}} |F_{X_t}(a^{H - H_0} x) - F_{X_t}(b^{H - H_0} x)| \\ &= \sup_{x \in \mathbb{R}} |F_{X_t}(\underline{a}^{H - H_0} x) - F_{X_t}(\overline{a}^{H - H_0} x)|. \end{aligned} \tag{7}$$

Remark 2.3. Eqs. (5), (6) and (7) are referred to the process X_t. Written for the (stationary) increments process $Z_{t,a} := X_{t+a} - X_t$ they become, respectively:

$$F_{Z_{t,a}}(x) := \mathbf{P}\left(Z_{t,a} < x\right) \overset{\text{by } H_0\text{-ss}}{=} \mathbf{P}\left(a^{H_0} Z_{t,1} < x\right) = F_{Z_{t,1}}(a^{-H_0} x),$$

$$F_{a^{-H} Z_{t,a}}(x) := \mathbf{P}\left(a^{-H} Z_{t,a} < x\right) \overset{\text{by } H_0\text{-ss}}{=} \mathbf{P}\left(a^{H_0 - H} Z_{t,1} < x\right) = F_{Z_{t,1}}(a^{H - H_0} x)$$

and

$$\delta_{Z_t}(\Psi_H) = \sup_{x \in \mathbb{R}} |F_{Z_{t,1}}(\underline{a}^{H - H_0} x) - F_{Z_{t,1}}(\overline{a}^{H - H_0} x)|.$$

The following Propositions are proved for $\delta(\Psi_H)$ by Bianchi [15]:

Proposition 2.1. *The process* $\{X_t, t \geq 0\}$ *is* H_0*-ss if and only if* $\delta_{X_t}(\Psi_{H_0}) = 0$.

Proposition 2.2. *Let* $\{X_t, t \geq 0\}$ *be* H_0*-ss. Then* $\delta_{X_t}(\Psi_H)$ *is non-increasing for* $H \leq H_0$ *and non-decreasing for* $H \geq H_0$.

Proposition 2.3. *Let* $\{X_t, t \geq 0\}$ *be* H_0*-ss,* $\mathbf{x} \geqq 0$ *or* $\mathbf{x} \leqq 0$, $\{\mathcal{A}_i\}_{i=1,\ldots,n}$ *be a sequence of timescale sets such that — denoted by* $\underline{a}_i = \min(\mathcal{A}_i)$ *and by* $\overline{a}_i = \max(\mathcal{A}_i)$*, with* $\underline{a}_i \leq \underline{a}_j$ *and* $\overline{a}_i \geq \overline{a}_j$ *for* $i > j$*, then, with respect to the sequence* $\{\mathcal{A}_i\}$*,* $\delta_{X_t}(\Psi_H)$ *is: (i) non-decreasing, if* $H \neq H_0$*; (ii) zero, if* $H = H_0$.

[3] In what follows we refer to process X, but – because of Remark 2.2 – the same results hold for the increments of X, provided of course that they are stationary.

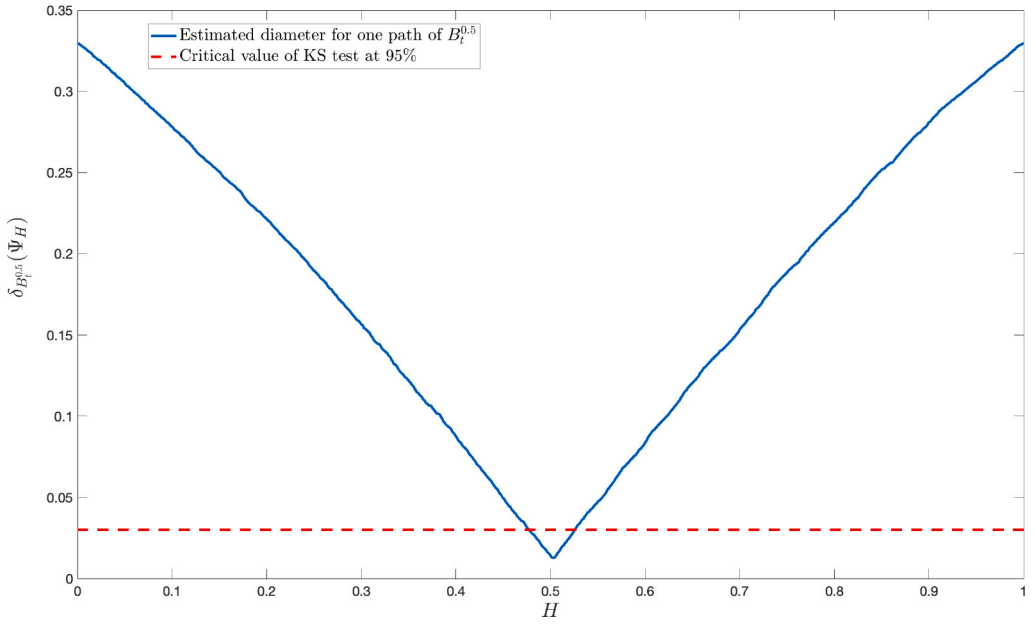

Fig. 1. Estimated diameter for only one path of Brownian motion ($H_0 = 0.5$) of length 4096, with $\underline{a} = 1$ and $\overline{a} = 25$. At the significance level $\alpha = 0.05$ the critical value of the Kolmogorov–Smirnov test is about 0.0301. The plot exhibits the minimum estimated diameter (about 0.0127) for $H_0 = 0.503$, corresponding to a p-value of about 0.8952. Given that the value of the minimum estimated diameter is smaller than the critical KS value, we accept self-similarity with parameter $\hat{H}_0 = 0.503$.

Proposition 2.4. *Let $\{B_t^{H_0}, t \geq 0\}$ be fractional Brownian motion of parameter H_0, with $\sigma^2 = \mathbb{E}(B_1^{H_0})$. Then*

$$\delta_{B_t^{H_0}}(\Psi_H) = \sup_{x \in \mathbb{R}} \frac{1}{\sigma\sqrt{2\pi}} \int_{x\underline{a}^{H-H_0}}^{x\overline{a}^{H-H_0}} e^{-u^2/2\sigma^2} du,$$

that is

$$\delta_{B_t^{H_0}}(\Psi_H) = \Phi(\hat{x}\overline{a}^{H_0-H}) - \Phi(\hat{x}\underline{a}^{H_0-H})$$

where Φ denotes the cumulative distribution function of a standard normal random variable and

$$\hat{x} = \begin{cases} \sqrt{\frac{2(H_0-H)}{\overline{a}^{2(H_0-H)} - \underline{a}^{2(H_0-H)}} \log\frac{\overline{a}}{\underline{a}}}, & \text{if } H \neq H_0 \\ 0, & \text{if } H = H_0. \end{cases}$$

Propositions 2.1 and 2.2 jointly entail that function $\delta_{X_t}(\Psi_H)$ of a non-degenerate self-similar process has a unique zero-valued minimum as a function of $H \in (0, 1]$, whose abscissa is attained precisely at H_0. Clearly, this mathematical statement must be turned into a statistical one, because – even for a genuine H_0-ss process – the empirical estimate of $\delta_{X_t}(\Psi_{H_0})$ does not necessarily return zero. Since the empirical diameter $\hat{\delta}_{X_t}(\Psi_H)$ reads as

$$\hat{\delta}_{X_t}(\Psi_H) = \max_{x \in \mathbb{R}} |\hat{F}_{X_1,n}(\underline{a}^H x) - \hat{F}_{X_1,m}(\overline{a}^H x)| \tag{8}$$

where $\hat{F}$ is the empirical cumulative distribution function

$$\hat{F}_{X_1,N}(a^H x) = \frac{1}{N}\sum_{i=1}^{N} \mathbb{1}_{X_{1,i} \leq a^H x},$$

the parameter H_0 should be estimated in practice as

$$\hat{H}_0 = \text{argmin}_{H \in (0,1]} \hat{\delta}_{X_t}(\Psi_H), \tag{9}$$

provided that $\hat{\delta}_{X_t}(\Psi_{\hat{H}_0})$ is statistically negligible. Fig. 1 provides an example of the estimated diameter for one path of Brownian motion.

Statistic (8) is precisely the two samples Kolmogorov–Smirnov (KS) metric, which evaluates the significance of the distance between the empirical cumulative distribution functions of two different i.i.d. samples of data. It is nonparametric, thus no assumption is made regarding the underlying distributions from which the samples are drawn.

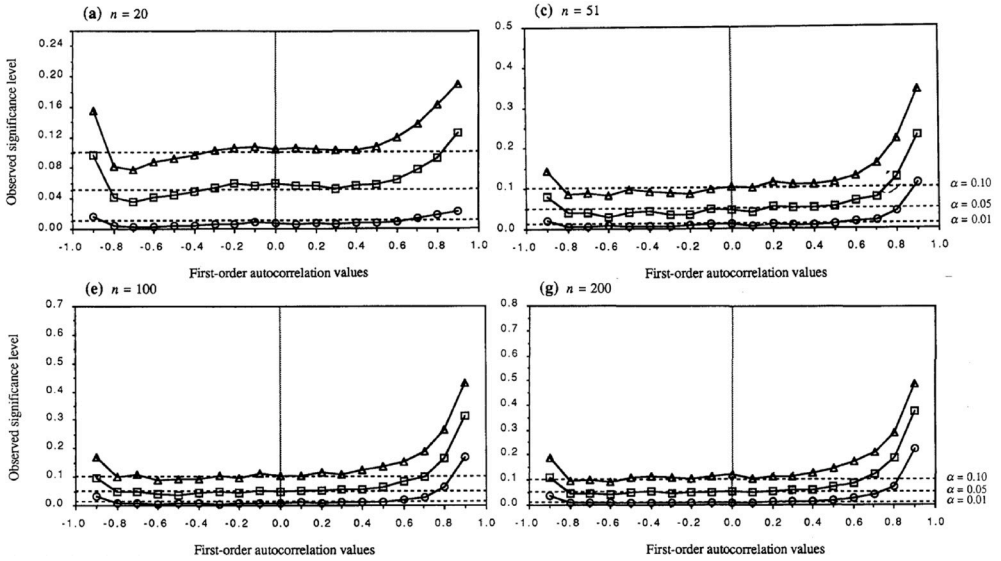

Fig. 2. Kolmogorov–Smirnov tests performed for simulated time series arising from a Gaussian AR(1) process: observed significance levels as a function of the first-order autocorrelation values. The nominal significance levels considered are: circles, $\alpha = 0.01$; squares, $\alpha = 0.05$; triangles $\alpha = 0.10$.
Source: Durilleul and Legendre [20].

3. Critical values of the KS test under fractional dependence

The only requirement which grounds relationship (8) is the statistical independence of the values within each sample. The violation of this assumption typically leads to rates of rejection or acceptance of the null hypothesis that deviate from the nominal ones. In the case of serially dependent data, Durilleul and Legendre [20] show that the KS statistic is too liberal for medium-to-high positively autocorrelated values and that for negatively autocorrelated values, the behavior is asymmetrical with respect to positive values. Thus, positive dependence leads to a reduction of the effective number of independent observations, even if the bias becomes negligible when the first-order autocorrelation is constrained to the interval $[-0.8, 0.3]$ and the number n of observations increases, see Fig. 2 reproduced from the study of Durilleul and Legendre [20]. If dependence more complex than the first or second-order autocorrelation is taken into account, excess rejection or excess acceptance of the null hypothesis affects statistic (8), depending on the sign of the dependence. For example, if the autocorrelation decays as a power law (as in the case of fBm), type I and type II errors[4] occur when $H > 1/2$ and $H < 1/2$, respectively.

Several remedies have been proposed in literature to face the dependence in data: Weiss [21] designs a procedure for data modeled by second-order auto-regressive (AR) processes with known parameters; Chicheportiche and Bouchaud [22] include all the lagged bivariate copulas, which encode the non-linear temporal dependences, and deduce some analytical results once the statistic is made parametric; Lanzante [23] tests three approaches for dealing with dependence and concludes that the best performance is achieved by a test based on Monte-Carlo simulations.

Beyond the rather articulated approach pursued by Chicheportiche and Bouchaud [22], to the authors' knowledge, the literature does not provide specific results (neither theoretical nor empirical) for the critical values of the KS statistic in the case of the rescaled distributions of fractional Brownian motion (or its increments). As the process is self-similar, we expect the rescaled distributions to be virtually indistinguishable, meaning that they exhibit a non-significant KS statistic. Since this problem is still unresolved from a theoretical standpoint due to its analytical complexity and nonlinearity, we design the following Monte-Carlo experiment with the aim to estimate the critical values of the test statistic depending on the sample sizes and the Hurst exponents, for different levels of significance:

(1) We simulated 1000 trajectories of fractional Brownian motion (fBm) of length n ($n = 256, 512, 1024, 2048, 4096, 16384$) and Hurst parameter H ($H = 0.1, \ldots, 0.9$; step 0.1);
(2) for each simulation, we estimated the self-similarity parameter and the corresponding minimum diameter of the increments' distributions, with a minimum timescale $\underline{a} = 1$ and maximum timescale $\overline{a} = 25$;
(3) we estimated the critical value (dependent on the value of H and the sample size n) for three confidence levels: the 90-th, 95-th, and 99-th percentiles of the distribution of the mimimal diameters;

[4] A type I error (false-positive) occurs when a null hypothesis that is actually true is rejected; a type II error (false-negative) occurs when a null hypothesis that is actually false is not rejected.

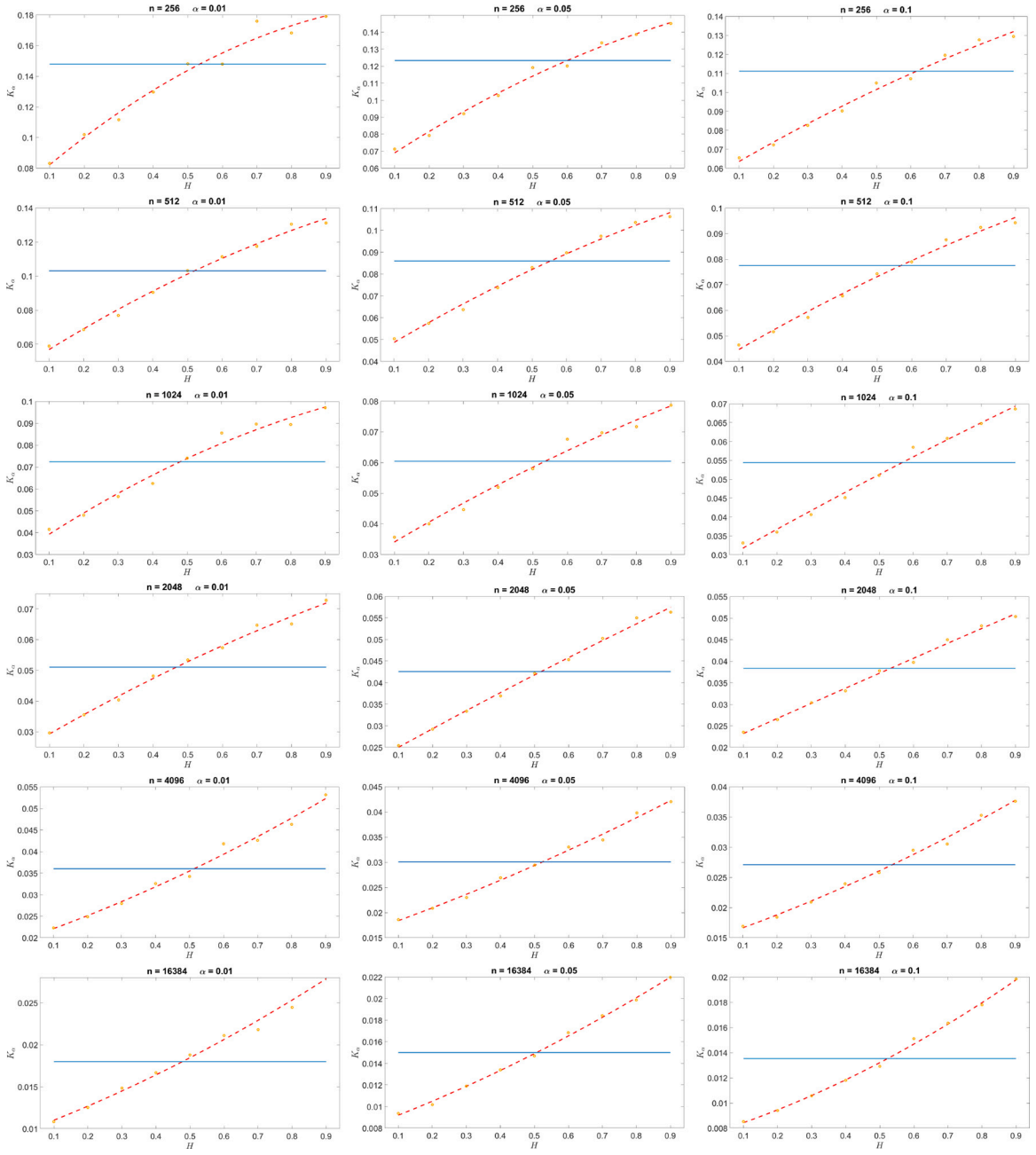

Fig. 3. Estimated critical values of the empirical KS statistic at 99-th (left column), 95-th (mid column) and 90-th (right column) percentile of 1000 simulated paths of fBm, for different sample sizes ($n = 256, 512, 1024, 2048, 4096, 16384$). The KS test was performed for the increments of each trajectory with $\underline{a} = 1$ and $\overline{a} = 25$; the empirical cumulative distributions of the minimal diameters served to calculate the three percentiles (orange circles). These values are compared with the critical value of the KS statistic in case of independence (blue solid line) and interpolated to get an approximate critical value for each value of H (red dotted line).

(4) driven by the visual inspection of data, we interpolated the values obtained in step (3) with a second-degree polynomial to obtain an estimate of the critical value for every possible value of H.

The results are summarized in Table 1 and Fig. 3. We observe a change in curvature (from concave to convex) in the interpolating polynomial as the sample size increases and (less evident) as the level of significance decreases. This behavior appears to be consistent with the effect of *long-term* memory, whose bias on the critical values of the KS statistic becomes more pronounced as the examined series becomes sufficiently long, since truncation errors in the simulated sequences become gradually less relevant.

Table 1
Parameters estimates of the interpolating polynomials for each sample size n and considered significance level α. The values in parentheses under the estimated coefficients c indicate the 95% confidence interval. In all cases the SSE (Sum of Squared Error) is between 0 and 0.0002.

	$P(H) = c_2 H^2 + c_1 H + c_0$			Goodness of fit		
	c_2	c_1	c_0	R-squared	Adj R-sq	RMSE
$n = 256$						
$\alpha = 0.01$	−0.0813	0.2028	0.0627	0.9740	0.9654	0.0063
	(−0.1697, 0.0072)	(0.1121, 0.2935)	(0.0429, 0.0825)			
$\alpha = 0.05$	−0.0426	0.1384	0.0557	0.9903	0.9870	0.0030
	(−0.0847, −0.0006)	(0.0952, 0.1815)	(0.0463, 0.0651)			
$\alpha = 0.10$	−0.0229	0.1083	0.0530	0.9892	0.9856	0.0028
	(−0.0622, 0.0164)	(0.0679, 0.1486)	(0.0443, 0.0618)			
$n = 512$						
$\alpha = 0.01$	−0.0365	0.1325	0.0440	0.9919	0.9892	0.0028
	(−0.0749, 0.0020)	(0.0931, 0.1719)	(0.0354, 0.0526)			
$\alpha = 0.05$	−0.0229	0.0971	0.0393	0.9946	0.9928	0.0017
	(−0.047, 0.0013)	(0.0723, 0.1218)	(0.0339, 0.0447)			
$\alpha = 0.10$	−0.0166	0.0812	0.0367	0.9913	0.9883	0.0019
	(−0.0434, 0.0102)	(0.0537, 0.1086)	(0.0307, 0.0427)			
$n = 1024$						
$\alpha = 0.01$	−0.0348	0.1075	0.0288	0.9810	0.9747	0.0032
	(−0.0796, 0.0100)	(0.0615, 0.1535)	(0.0188, 0.0389)			
$\alpha = 0.05$	−0.0133	0.0689	0.0273	0.9852	0.9803	0.0022
	(−0.0433, 0.0166)	(0.0381, 0.0996)	(0.0206, 0.0340)			
$\alpha = 0.10$	−0.0043	0.0513	0.0267	0.9904	0.9872	0.0015
	(−0.0247, 0.0161)	(0.0304, 0.0722)	(0.0221, 0.0312)			
$n = 2048$						
$\alpha = 0.01$	−0.0139	0.0672	0.0227	0.9925	0.9901	0.0015
	(−0.0343, 0.0065)	(0.0463, 0.0881)	(0.0182, 0.0273)			
$\alpha = 0.05$	−0.0034	0.0440	0.0207	0.9954	0.9939	0.0009
	(−0.0156, 0.0087)	(0.0315, 0.0565)	(0.0171, 0.0234)			
$\alpha = 0.10$	−0.0006	0.0353	0.0197	0.9955	0.9940	0.0007
	(−0.0109, 0.0097)	(0.0247, 0.0459)	(0.0174, 0.0220)			
$n = 4096$						
$\alpha = 0.01$	0.0107	0.0270	0.0193	0.9860	0.9814	0.0014
	(−0.0091, 0.0305)	(0.0067, 0.0473)	(0.0149, 0.0238)			
$\alpha = 0.05$	0.0061	0.0238	0.0160	0.9938	0.9917	0.0007
	(−0.0043, 0.0165)	(0.0131, 0.0344)	(0.0136, 0.0183)			
$\alpha = 0.10$	0.0072	0.0191	0.0147	0.9935	0.9913	0.0007
	(−0.0022, 0.0167)	(0.0095, 0.0288)	(0.0126, 0.0168)			
$n = 16384$						
$\alpha = 0.01$	0.0061	0.0150	0.0095	0.9874	0.9832	0.0008
	(−0.0044, 0.0166)	(0.0042, 0.0257)	(0.0071, 0.0118)			
$\alpha = 0.05$	0.0043	0.0116	0.0080	0.9981	0.9975	0.0002
	(0.0013, 0.0074)	(0.0085, 0.0148)	(0.0073, 0.0087)			
$\alpha = 0.10$	0.0057	0.0085	0.0075	0.9975	0.9966	0.0002
	(0.0025, 0.0088)	(0.0053, 0.0118)	(0.0068, 0.0082)			

Assuming that realized log-volatility behaves like a fractional Ornstein–Uhlenbeck process, we exploit its stationarity to de-Lampertize it through transform (4). Once the process is converted into a self-similar sequence, we estimate its parameter by the KS test. In this regard, two issues deserve to be mentioned:

- when one deals with real data, the self-similarity parameter of X_t is not known in advance, so the Lamperti transform (4) can be computed with any $H \in (0, 1]$. In the next Section, it will be shown that the self-similarity parameter of X_t: (a) does not depend on the value of H chosen to apply transform (4) (Proposition 4.1), indeed using different parameters in relation (4) can help stabilize the estimate of the self-similarity parameter; (b) is equal to the parameter of the fBm driving the fractional Ornstein–Uhlenbeck (fOU1) process, when this is the solution of the Langevin equation (Proposition 4.2).
- In Section 5, the empirical autocorrelation functions of the increments of the de-Lampertized sequences X_t will be calculated to evaluate whether the standard critical values of the KS test can be used to evaluate the significance of the estimated minimal diameters, according to the findings of Durilleul and Legendre [20]. Given the sizes of the samples that we will investigate (thousands of observations), we expect that no correction will be necessary for the critical values of the KS test.

4. Fractional Ornstein–Uhlenbeck and its Lamperti transform

Studying the smoothness of the volatility process at high frequencies, Gatheral et al. [1] argue that the logarithm of realized volatility behaves at any reasonable timescale as a fBm with Hurst exponent H of order 0.1. On the strength of these empirical observations, they propose the stationary *Rough Fractional Stochastic Volatility* (RFSV) model defined by the system

$$\begin{cases} dS_t = \mu_t S_t dt + S_t \sigma_t dB_t \\ \sigma_t = \exp(V_t) \end{cases}$$

where S_t is the stock price, μ_t is the drift, B_t is the Brownian motion and the logarithm of the volatility σ_t is modeled by a fractional Ornstein–Uhlenbeck (fOU) process V_t.

This process can be constructed in different ways. Lim and Muniandy [24] consider three types of fOU process: the stationary process obtained by the Lamperti transform of the fBm, the process with stretched exponential covariance and the process obtained by solving the fractional Langevin equation.[5] Similarly, Cheridito et al. [25] and Kaarakka and Salminen [26],Kaarakka [27] study two types of fOU process: the stationary solution of the Langevin equation driven by a fractional Brownian motion (fOU1), and the stationary process obtained by applying the Lamperti transform (3) to the fractional Brownian motion (fOU2). Unlike what happens for the ordinary OU process (for which the two routes provide the same process), the autocovariance of fOU1 decays like that of a power function, whereas the autocovariance of fOU2 decays exponentially. This difference is not relevant for our analysis, because in both cases the process obtained from the Lamperti transform (4) is self-similar with a parameter equal to that of the fBm driving the Langevin equation (fOU1) (see Proposition 4.2) or to the parameter of the fBm in the inverse Lamperti transformation (3) (by definition). An analysis involving the behavior and the estimation of the Hurst parameter with the Lamperti transform of an fBm can be found in [28], where it is stated that the perceived Hurst exponent underestimates the Hurst exponent of the underlying fBm. In this regard, the (nonparametric) distribution-based method that we propose to estimate the roughness of the log-volatility is more robust with respect to other techniques based on the scaling of individual moments, which are affected by the characteristics of the autocovariance functions and may therefore result in different estimates depending on which alternative is considered (fOU1 or fOU2).

4.1. Fractional Ornstein–Uhlenbeck of type 1 (fOU1)

Let us consider the linear stochastic differential equation (Langevin-like equation) driven by an fBm of parameter H_0

$$dV_t = -\alpha V_t dt + dB_t^{H_0}, \quad t \geq 0, \tag{10}$$

with $\alpha > 0$. The solution of this equation is

$$V_t = e^{-\alpha t}\left(V_0 + \int_0^t e^{\alpha s} dB_s^{H_0}\right)$$

where the initial value $V_0 := \int_{-\infty}^0 e^{\alpha s} d\widehat{B}_s^{H_0}$ with $\widehat{B}_t^{H_0}$ a two-sided fBm.[6] In general, for every $V_0 \in L^0(\Omega)$, V_t is called a *fractional Ornstein–Uhlenbeck process (fOU1) with initial condition* V_0.

Cheridito et al. [25] (Theorem 2.3, p.7) show that the pathwise Riemann–Stieltjes integral exists and that, for $H \in (0, 1/2) \cup (1/2, 1]$, $N = 1, 2, \ldots$, $t \in \mathbb{R}$ fixed and $s \to \infty$ the covariance of V_t is

$$\mathrm{Cov}(V_t, V_{t+s}) = \frac{1}{2}\sum_{n=1}^{N} \alpha^{-2n}\left(\prod_{k=0}^{2n-1}(2H-k)\right) s^{2H-2n} + \mathcal{O}\left(s^{2H-2N-2}\right).$$

The decay of $\mathrm{Cov}(V_t, V_{t+s})$ is very similar to the decay of $\mathrm{Cov}(B_{h+t}^H - B_h^H, B_{h+s+t}^H - B_{h+s}^H)$ and exhibits short-range dependence if $H < 1/2$ and long-range dependence if $H > 1/2$.

The following two Propositions ensure that the self-similarity parameter of X_t in relation (4): (a) does not depend on the value $H \in (0, 1]$ chosen to calculate the Lamperti transform and (b) equals the parameter of the fBm which drives the fOU1, solution of the Langevin equation.

Proposition 4.1. *Let $\{Y_t, t \in \mathbb{R}^+\}$ be strictly stationary. Then, for any $H \in (0, 1]$, there exists a unique $H_0 \in (0, 1]$ such that the Lamperti transform $X_t = t^H Y_{\log t}$ is H_0-ss.*

[5] Actually, the fractional Langevin equation considered by Lim and Muniandy [24] is different from the one discussed by the more quoted paper of Cheridito et al. [25]. The former discuss the not-easy-to-manage solutions of the two 'fractionalized' Langevin equations: $\frac{d^\beta Y_t}{dt^\beta} + aY_t = W_t$ or $\left(\frac{d}{dt} + a\right)^\beta Y_t = W_t$, where β is the order of the fractional derivative. The latter do not fractionalize the order of differentiation, but replace the Brownian motion by the fractional Brownian motion, as will be more closely illustrated in the following.

[6] The two-sided fBm can be defined letting ${}^{(-)}B_t^{H_0}$ be a fractional Brownian motion independent on $B_t^{H_0}$ and setting

$$\widehat{B}_t^{H_0} = \begin{cases} B_t^{H_0}, & t \geq 0 \\ {}^{(-)}B_{-t}^{H_0}, & t < 0 \end{cases}$$

Proof. From the Lamperti transform one has

$$X_t = t^H Y_{\log t} \quad \text{and} \quad X_{at} = (at)^H Y_{\log at}.$$

By definition, X_t is self-similar of parameter H_0 if $\{a^{H_0} X_t\} \overset{d}{=} \{X_{at}\}$, that is

$$\{a^{H_0} t^H Y_{\log t}\} \overset{d}{=} \{a^H t^H Y_{\log at}\}$$

The factor t^H can be canceled and this entails that the choice of H in Eq. (4) does not affect the self-similarity parameter H_0. In fact,

$$\{a^{H_0} Y_{\log t}\} \overset{d}{=} \{a^H Y_{\log a + \log t}\}.$$

By the stationarity of Y_t, $\{Y_{\log a+\log t}\} \overset{d}{=} \{Y_{\log t}\}$, therefore

$$\{a^{H_0} Y_{\log t}\} \overset{d}{=} \{a^H Y_{\log t}\}$$

if and only if $H = H_0$, whatever t^H is considered in the Lamperti transform. □

Proposition 4.2. *The Lamperti transform (4) of the fOU1 process driven by a fBm of parameter H_0 is H_0-ss.*

Proof. Without loss of generality, we set $V_0 = 0$, so that

$$V_t = e^{-\alpha t} \int_0^t e^{\alpha s} d B_s^{H_0}.$$

For any H, we have to prove that equality (1) holds with $X_t = t^H V_{\log t}$, that is $X_{at} \overset{d}{=} a^{H_0} X_t$. It is

$$\begin{aligned} X_{at} &= (at)^H V_{\log(at)} \\ &= (at)^H e^{-\alpha \log(at)} \int_0^{\log(at)} e^{\alpha s} d B_s^{H_0} \\ &= (at)^{H-\alpha} \int_0^{\log(at)} e^{\alpha s} d B_s^{H_0} \end{aligned} \tag{11}$$

and

$$\begin{aligned} a^{H_0} X_t &= a^{H_0} t^H V_{\log(t)} \\ &= a^{H_0} t^H e^{-\alpha \log t} \int_0^{\log t} e^{\alpha s} d B_s^{H_0} \\ &= a^{H_0} t^{H-\alpha} \int_0^{\log t} e^{\alpha s} d B_s^{H_0}. \end{aligned} \tag{12}$$

Equating in distribution (11) and (12), we have

$$a^{H-\alpha} \int_0^{\log(at)} e^{\alpha s} d B_s^{H_0} \overset{d}{=} a^{H_0} \int_0^{\log t} e^{\alpha s} d B_s^{H_0}. \tag{13}$$

Let us prove that the above equality holds if and only if $H = H_0$. If this equality is true, then simplifying (13) we have

$$\int_0^{\log(at)} e^{\alpha s} d B_s^{H_0} \overset{d}{=} a^{\alpha} \int_0^{\log t} e^{\alpha s} d B_s^{H_0}. \tag{14}$$

Setting $v = s + \log a$ yields to

$$\int_0^{\log(at)} e^{\alpha s} d B_s^{H_0} \overset{d}{=} a^{\alpha} \int_{\log a}^{\log(at)} e^{\alpha(v-\log a)} d B_{v-\log a}^{H_0}$$

$$\int_0^{\log(at)} e^{\alpha s} d B_s^{H_0} \overset{d}{=} a^{\alpha} \int_{\log a}^{\log(at)} e^{\alpha v} a^{-\alpha} d B_{v-\log a}^{H_0}.$$

Since $d B_{v-\log a}^{H_0} \overset{d}{=} d B_v^{H_0}$ and V is a stationary process as well, we finally have

$$\int_0^{\log(at)} e^{\alpha s} d B_s^{H_0} \overset{d}{=} \int_0^{\log t} e^{\alpha v} d B_v^{H_0}. \tag{15}$$

Thus, process X_t is self-similar with parameter H_0. The necessary condition follows from the uniqueness of the self-similarity parameter. □

4.2. Fractional Ornstein–Uhlenbeck of type 2 (fOU2)

A different type of fractional Ornstein–Uhlenbeck process can be constructed starting from the Lamperti transform (3) with $X = B^H$. Following Kaarakka [27], one can first of all consider the Ornstein–Uhlenbeck process defined in terms of Brownian motion B as

$$U_t = e^{-\alpha t} B_{\frac{1}{2\alpha} e^{2\alpha t}} \quad (\alpha > 0, t \in \mathbb{R}).$$

It follows that

$$\begin{aligned} dU_t &= -\alpha e^{-\alpha t} B_{\frac{1}{2\alpha} e^{2\alpha t}} dt + e^{-\alpha t} dB_{\frac{1}{2\alpha} e^{2\alpha t}} \\ &= -\alpha U_t dt + e^{-\alpha t} dB_{\frac{1}{2\alpha} e^{2\alpha t}}, \end{aligned} \tag{16}$$

with $\int_0^t e^{-\alpha s} dB_{\frac{1}{2\alpha} e^{2\alpha s}}$ be the Brownian motion (the results directly follows from the Lévy's characterization theorem). To generalize Eq. (16) to the fBm of parameter $H \in (0, 1]$ one can consider the pathwise Riemann–Stieltjes integral

$$U_t^{(\alpha)} = \int_0^t e^{-\alpha s} dB^H_{\frac{H}{\alpha} e^{\frac{\alpha}{H} s}}, \tag{17}$$

and recognize that transform (3) with $X = B^H$ is a solution of the linear SDE

$$dV_t = -\alpha V_t dt + dU_t^{(\alpha)}$$

with initial value

$$V_0 = B^H_{\frac{H}{\alpha}} \sim \mathcal{N}\left(0, \left(\frac{H}{\alpha}\right)^{2H}\right).$$

Since it can be proved that for any $\alpha > 0$ and $t \geq 0$

$$\{\alpha^H U^{(\alpha)}_{t/\alpha}\} \overset{d}{=} \{U_t^{(1)}\}$$

a new Langevin stochastic differential equation can be defined having as driving process the two-sided version $\hat{U}^{(1)}$ of $U^{(1)}$, i.e.

$$dL_t = -\gamma L_t dt + dU_t^{(1)}, \ \gamma > 0.$$

The solution of this equation,

$$L_t = e^{-\gamma t} \int_{-\infty}^t e^{\gamma s} d\hat{U}_s^{(1)} = e^{-\gamma t} \int_{-\infty}^t e^{(\gamma - 1)s} dB^H_{He^{\frac{s}{H}}}, \ \gamma > 0,$$

is called *fractional Ornstein–Uhlenbeck process of type 2* (fOU2).

L_t is locally Hölder continuous of any order $\beta < H$, but – unlike fOU1 – it is short range dependent. In fact, it can be shown that for $H \in \left(\frac{1}{2}, 1\right)$ the covariance kernel of L_t reads as

$$\mathbb{E}\left(L_t L_s\right) = (2H-1) H^{2H-1} e^{-\gamma(t+s)} \int_{-\infty}^t \int_{-\infty}^s \frac{e^{\left(\gamma - 1 + \frac{1}{H}\right)(u+v)}}{\left|e^{\frac{u}{H}} - e^{\frac{v}{H}}\right|^{2(1-H)}} du dv$$

and decreases exponentially as [see [27]]

$$\mathbb{E}\left(L_t L_s\right) = \mathcal{O}\left(e^{-\min\left\{\gamma, \frac{1-H}{H}\right\} t}\right), \text{ as } t \to \infty.$$

Even though the process is fractional, the fOU2 allows for greater analytical tractability: for example, the quick decay of the autocorrelation could justify the use of the KS test in its standard form, without essential corrections due to the dependence in data. Nonetheless, for volatility modeling purposes, fOU1 is the specification generally considered.

5. Data analysis

In this section, we discuss the results of the estimations of the self-similarity parameters for both simulated fOU1 processes and realized volatilities of 21 stock indices. The fOU1 trajectories, of length $n = 5,000$, were simulated by generating fractional Gaussian noises using the Wood and Chan [29] algorithm as implemented in Fraclab 2.2 Toolbox provided by INRIA. The self-similarity parameters of the realized volatilities were estimated using the 5-minute realized variance data released by the Oxford-Man Institute's Realized Library. Data cover the period from January 3, 2000 to June 27, 2018 and relate to the 21 stock indices listed in Table 2.

First, the validity of Propositions 4.1 and 4.2 is established by showing that the Lamperti transform X_t of a fOU process driven by a fBm with parameter H_0, is itself H_0-ss, regardless of the parameter H used in the transform (4). To do this, the surrogated fOU1 was de-Lampertized by applying transform (4) with any parameter $H \in (0, 1)$ with a step of 0.01. Then, with the set of timescales

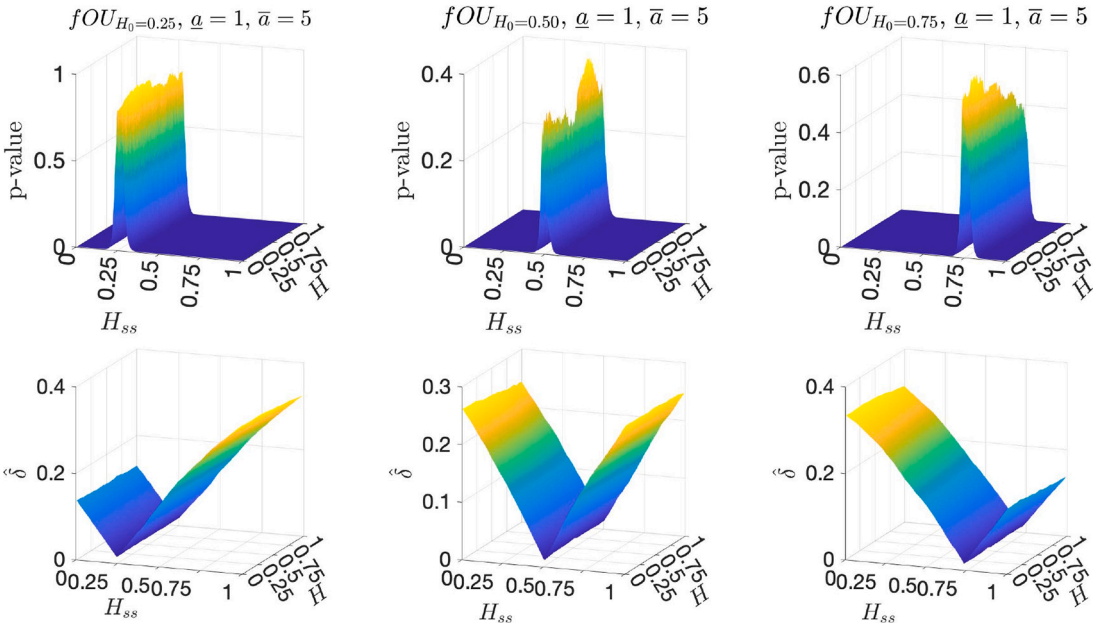

Fig. 4. (Bottom panels) KS tests for three simulated fOU1 of length $n = 5,000$, with prescribed $H_0 = \{0.25, 0.5, 0.75\}$. The diameter $\hat{\delta}_{Z_t}(\Psi_{H_{ss}})$ is reported as a function of the Lamperti transform parameter $H \in (0, 1]$, with step 0.01, and of the candidate self-similarity parameter $H_{ss} \in (0, 1]$, with step 0.0001. (Top panels) p-values of the KS tests as a function of H and H_{ss}. The minimum $\hat{\delta}$ (maximum p-value) is achieved precisely when H_{ss} equals the self-similarity parameter H_0 prescribed for the fBm driving the simulated fOU1, regardless the value H used to calculate the Lamperti transform (4). The set of timescales used is $\mathcal{A} = [\![1, 5]\!]$.

$\mathcal{A} = [\![1, 5]\!]$ fixed, for each potential self-similarity parameter $H_{ss} \in (0, 1)$ with a step of 0.0001, the distance $\hat{\delta}(\Psi_{H_{ss}})$ between the empirical distributions $\hat{F}_{Z_{t,1}}(x)$ and $\hat{F}_{Z_{t,1}}(5^{-H_{ss}}x)$ was calculated using Eq. (8), where $Z_{t,1} = X_{t+1} - X_t$. This process was iterated for all H_{ss} and H. The reason why the distributions are calculated only for $\underline{a}$ and $\overline{a}$ lies in Proposition 2.3, stating that – if the process is H_0-ss – the diameter is constant for $H = H_0$ and non decreasing with $\overline{a}_i$ for values of H other than H_0. Thus the worst case is given by maximizing the distance between timescales; this has also the advantage to greatly reduce the amount of computations required to test self-similarity.

Fig. 4 shows the implementation of the previous procedure for three fOU1 samples with prescribed $H_0 = \{0.25, 0.5, 0.75\}$ and timescales set $\mathcal{A} = [\![1, 5]\!]$.

The top panels show the p-values of the KS tests while the bottom panels display the surfaces $\hat{\delta}$, both as functions of H and H_{ss}. In all cases, the minima of $\hat{\delta}$ (or the maxima of the p-values) are the images of values $\hat{H}_0$ very close to the prescribed H_0 of the starting fOU1 trajectories, regardless the value of H used in the Lamperti transform. For each $H \in (0, 1)$ step 0.01, we estimate $\hat{H}_0$ as the value which minimizes the diameter $\hat{\delta}$; the mean value over the 100 values of H used in transform (4) provides the final estimate. The estimated self-similarity exponents are $\hat{H}_0 = \{0.2592 \pm 0.0036, 0.4978 \pm 0.0041, 0.7572 \pm 0.0044\}$, where the error is measured through the standard deviation of the estimates over the 100 simulations; these values indicate that the Lamperti transform of a fOU process driven by a fBm with parameter H_0 is itself H_0-ss, whatever the value of H_0 and whatever the value of H which is used in the Lamperti transform. In addition, the methodology described in the previous sections seems very effective in accurately identifying the self-similarity parameter.

Assuming that $\log \sigma_t$ computed from the realized variance follows a fOU process as in Eq. (10), the stationarity of the data was tested using the Augmented Dickey–Fuller test (ADF) on the null model

$$\log \sigma_t = \beta_0 + \log \sigma_{t-1} + \lambda_1 \Delta \log \sigma_{t-1} + \lambda_2 \Delta \log \sigma_{t-2} + \cdots + \lambda_k \Delta \log \sigma_{t-k} + \epsilon_t$$

against the alternative one

$$\log \sigma_t = \beta_0 + \alpha \log \sigma_{t-1} + \lambda_1 \Delta \log \sigma_{t-1} + \lambda_2 \Delta \log \sigma_{t-2} + \cdots + \lambda_k \Delta \log \sigma_{t-k} + \epsilon_t$$

with drift coefficient β_0, AR(1) coefficient $\alpha < 1$, and $\epsilon_t \sim NID(0, 1)$. As usual, Δ denotes the differencing operator ($\Delta \log \sigma_t = \log \sigma_t - \log \sigma_{t-1}$) and k is the number of lagged difference terms. The two rightmost columns of Table 2 report the value and the p-value of the ADF statistic, which for all indexes is smaller than the critical value, meaning that stationary for $\log \sigma_t$ cannot be rejected.

Since the self-similarity parameter is estimated by calculating diameter (8) for the increments $Z_{t,a} := X_t - X_{t-a}$, $a \in \mathcal{A}$, of the transformed process X_t, first and foremost, we verified the stationarity $Z_{t,a}$ using the ADF test with a null model

$$Z_{t,1} = \beta_0 + Z_{t-1,1} + \lambda_1 \Delta Z_{t-1,1} + \lambda_2 \Delta Z_{t-2,1} + \cdots + \lambda_k \Delta Z_{t-k,1} + \epsilon_t$$

Table 2
The first two columns report the 21 tickers and indices examined. The third column shows the number of observations for each index. Finally, the two rightmost columns report the ADF statistic and the related p-values.

Ticker	Index	Obs.	ADF	p-value
SPX	Standard & Poor 500 (USA)	4641	−14.390	<0.001
FTSE	Footsie 100 (GBR)	4660	−15.886	<0.001
N225	Nikkei 225 (JPN)	4501	−16.238	<0.001
GDAXI	Dax 30 (DEU)	4692	−14.267	<0.001
RUT	Russell 2000 (USA)	4636	−18.909	<0.001
AORD	All Ordinaries (AUS)	4665	−18.861	<0.001
DJI	Dow Jones I. (USA)	4635	−15.354	<0.001
IXIC	Nasdaq C. (USA)	4637	−13.526	<0.001
FCHI	Cac 40 (FRA)	4713	−14.405	<0.001
HSI	Hang Seng I. (HKG)	4532	−15.611	<0.001
KS11	Kospi C. I. (KOR)	4550	−11.902	<0.001
AEX	Amsterdam Exchange I. (NLD)	4714	−13.850	<0.001
SSMI	Swiss Market I. (CHE)	4636	−13.219	<0.001
IBEX	Ibex 35 (ESP)	4681	−14.458	<0.001
NSEI	Nifty 50 (IND)	4586	−15.644	<0.001
MXX	Mexico Stock Exchange (MEX)	4640	−19.473	<0.001
BVSP	Bovespa I. (BRA)	4556	−19.268	<0.001
GSPTSE	Toronto Stock Exchange C. I. (CAN)	4043	−15.314	<0.001
STOXX50E	Euro Stock 50 (EUR)	4713	−17.973	<0.001
FTSTI	Straits Times I. (SGP)	2696	−16.045	<0.001
FTSEMIB	Milano Indice di Borsa (ITA)	2307	−13.069	<0.001

Table 3
The ADF statistics and the p-values for the increments $Z_{t,1}$ of the Lamperti transform of $\log \sigma_t$ with $H = \overline{\hat{H}_0}$, as reported in Table 5 for each examined index.

Ticker	ADF	p-value	Ticker	ADF	p-value	Ticker	ADF	p-value
SPX	−70.445	<0.001	IXIC	−68.432	<0.001	NSEI	−75.359	<0.001
FTSE	−74.268	<0.001	FCHI	−72.844	<0.001	MXX	−74.510	<0.001
N225	−69.858	<0.001	HSI	−76.352	<0.001	BVSP	−70.117	<0.001
GDAXI	−74.407	<0.001	KS11	−70.493	<0.001	GSPTSE	−69.420	<0.001
RUT	−72.623	<0.001	AEX	−72.336	<0.001	STOXX50E	$-77.253t$	<0.001
AORD	−78.525	<0.001	SSMI	−71.929	<0.001	FTSTI	−58.243	<0.001
DJI	−72.912	<0.001	IBEX	−72.401	<0.001	FTSEMIB	−50.403	<0.001

against the alternative one

$$Z_{t,1} = \beta_0 + \alpha Z_{t-1,1} + \lambda_1 \Delta Z_{t-1,1} + \lambda_2 \Delta Z_{t-2,1} + \cdots + \lambda_k \Delta Z_{t-k,1} + \epsilon_t.$$

For this purpose, given that the choice of the parameter H in the Lamperti transformation is irrelevant (Propositions 4.1 and 4.2) and hence it is not necessary to repeat the test for all $H \in (0,1)$ step 0.01, increments were calculated for the sequences X_t obtained using the self-similarity parameter H_0 estimated for each stock index, as reported in Table 5. Table 3 displays the value and the p-value of the ADF tests. Also in this case we obtained for all indexes an ADF statistic smaller than the critical value. Furthermore, we cannot reject stationarity even for values of $H \neq 0.1$.

In order to verify whether the critical values of the KS statistic can apply to the examined dataset, the autocorrelations were calculated for both the 21 indexes and the simulated fOU1 processes with prescribed $H_0 = \{0.25, 0.50, 0.75\}$. Table 4 displays the autocorrelations up to lag 5; with the exception of $fOU1_{H=075}$, the values for all the remaining lags are not significantly different from zero (this can be explained by the fact that $fOU1_{H=075}$ is the only one with long memory). In particular, for all indexes, we observe large first-order autocorrelation, while the following orders are negligible. Furthermore, considering that all series have lengths $n > 2300$, we can evaluate the significance of the diameter using the critical values of the KS statistic for our dependent data, in the light of the results of Durilleul and Legendre [20] discussed in Section 2. On the strength of the results obtained in the previous analyses, we proceeded to estimate the self-similarity exponent $\hat{H}_0$ of each stock index as the point of minimum of the diameter, provided that this is statistically negligible. As for the simulated fOU1 sequences, the diameter was calculated for the distributions of the increments of the process X_t, obtained using different Lamperti parameters H and self-similarity parameters H_{ss}.

Using the SPX index as an example, the top panels of Fig. 5 display the p-values of the KS tests (left) and the estimated diameters (right), both with respect to H and H_{ss}. The bottom left panel shows the values $\hat{H}_0$ estimated for a fOU process with $H_0 = 0.10$ for increasing $\bar{a} \in [\![2, 20]\!]$. The values are dispersed around the prescribed H_0 with a mean of 0.096 ± 0.003. This leads us to choose the mean over the set of upper timescales $\bar{a}$ as the best estimate $\overline{\hat{H}_0}$. The bottom right panel shows the same analysis for the log-volatility of the SPX index with an estimated $\overline{\hat{H}_0} = 0.142 \pm 0.009$. We observe that the real data exhibit a slightly larger spread compared to the simulated fOU process. This analysis was performed for each index and Table 5 summarizes the estimates $\overline{\hat{H}_0}$ averaged on upper timescales $\bar{a} \in [\![2, 20]\!]$. In every instance, we find notably low values for the self-similarity parameter, i.e. low Hurst exponents

Table 4
First five-order autocorrelations for both indexes and fOU1 processes. Since most of the indices display estimated self-similarity parameters close to 0.1 (see Table 5), we also reported the autocorrelations for the $fOU1_{H=0.1}$ process.

	1st lag	2nd lag	3rd lag	4th lag	5th lag
SPX	−0.4017	−0.0142	−0.0339	0.0078	−0.0029
FTSE	−0.4336	−0.0118	−0.0308	−0.0007	0.0131
N225	−0.3715	−0.0565	−0.0018	−0.0421	0.0165
GDAXI	−0.3999	−0.0550	0.0127	−0.0513	0.0492
RUT	−0.4072	−0.0319	−0.0269	0.0137	−0.0105
AORD	−0.4802	0.0131	−0.0313	0.0419	−0.0412
DJI	−0.4338	0.0003	−0.0313	0.0146	−0.0121
IXIC	−0.3414	−0.0629	−0.0478	0.0178	−0.0054
FCHI	−0.3887	−0.0505	−0.0080	−0.0474	0.0756
HSI	−0.4620	−0.0020	0.0075	−0.0149	−0.0245
KS11	−0.4065	−0.0161	−0.0194	−0.0320	0.0019
AEX	−0.3855	−0.0483	−0.0124	−0.0453	0.0655
SSMI	−0.3863	−0.0501	−0.0054	−0.0223	0.0319
IBEX	−0.3753	−0.0650	−0.0079	−0.0351	0.0576
NSEI	−0.4111	−0.0567	0.0238	−0.0152	0.0129
MXX	−0.4528	0.0104	−0.0268	−0.0276	0.0245
BVSP	−0.3752	−0.0503	−0.0499	0.0003	0.0365
GSPTSE	−0.4527	0.0116	−0.0051	−0.0494	0.0160
STOXX50E	−0.4172	−0.0594	0.0202	−0.0308	0.0261
FTSTI	−0.4627	0.0072	−0.0306	0.0012	0.0002
FTSEMIB	−0.3764	−0.0573	−0.0070	−0.0528	0.0858
$fOU1_{H=0.10}$	−0.4463	0.0154	−0.0397	−0.0097	0.0038
$fOU1_{H=0.25}$	−0.2979	−0.0487	−0.0059	−0.0414	0.0072
$fOU1_{H=0.50}$	−0.0143	−0.0096	−0.0061	−0.0186	0.0077
$fOU1_{H=0.75}$	0.4084	0.2724	0.2234	0.1858	0.1816

Table 5
For each index the estimate $\overline{\hat{H}_0}$ is reported. The values are averaged with respect to an increasing upper timescale, i.e. $\underline{a} = 1$ and $\overline{a} \in [\![2, 20]\!]$. For AORD the exact p-value is 0.997 ± 0.003.

Ticker	$\overline{\hat{H}_0}$	$\hat{\delta}$	p-value	Ticker	$\overline{\hat{H}_0}$	$\hat{\delta}$	p-value
SPX	0.142 ± 0.009	0.015 ± 0.001	0.67 ± 0.04	AEX	0.139 ± 0.014	0.020 ± 0.002	0.30 ± 0.10
FTSE	0.110 ± 0.011	0.015 ± 0.001	0.71 ± 0.09	SSMI	0.117 ± 0.008	0.014 ± 0.002	0.73 ± 0.11
N225	0.133 ± 0.008	0.011 ± 0.001	0.94 ± 0.04	IBEX	0.137 ± 0.025	0.024 ± 0.002	0.14 ± 0.05
GDAXI	0.133 ± 0.011	0.017 ± 0.001	0.49 ± 0.09	NSEI	0.130 ± 0.013	0.013 ± 0.007	0.86 ± 0.05
RUT	0.122 ± 0.008	0.012 ± 0.007	0.91 ± 0.03	MXX	0.091 ± 0.009	0.011 ± 0.001	0.95 ± 0.03
AORD	0.060 ± 0.010	0.008 ± 0.005	1.00 ± 0.00	BVSP	0.137 ± 0.015	0.015 ± 0.001	0.70 ± 0.10
DJI	0.112 ± 0.017	0.023 ± 0.001	0.16 ± 0.04	GSPTSE	0.087 ± 0.008	0.010 ± 0.001	0.97 ± 0.03
IXIC	0.151 ± 0.011	0.014 ± 0.002	0.75 ± 0.16	STOXX50E	0.147 ± 0.012	0.017 ± 0.001	0.53 ± 0.09
FCHI	0.117 ± 0.030	0.028 ± 0.002	0.05 ± 0.02	FTSTI	0.067 ± 0.011	0.025 ± 0.003	0.39 ± 0.16
HSI	0.071 ± 0.009	0.011 ± 0.001	0.93 ± 0.05	FTSEMIB	0.122 ± 0.021	0.035 ± 0.003	0.13 ± 0.05
KS11	0.113 ± 0.013	0.018 ± 0.002	0.49 ± 0.13				

for the log-volatility. Our findings are in robust agreement with the results presented in [1], further substantiating the notion that log-volatility exhibits rough trajectories.

6. Conclusion

Our analysis focuses on estimating the self-similarity exponents of the Lamperti transforms of log-volatilities for 21 stock indices. We propose an innovative methodology that differs from the conventional approaches typically employed for estimating the Hurst exponent of the volatility process. Specifically, we relate the estimation of the roughness parameter to that of the self-similarity exponent of the process obtained through the Lamperti transform of volatility, and assess the statistical significance of the resulting estimates using the Kolmogorov–Smirnov test. Our analysis of the 21 stock indices, which has proven effective even when benchmarked against the fractional Ornstein–Uhlenbeck process, is consistent with the findings that the volatility is indeed rough. We observed values of the Hurst parameter ranging from 0.06 for the Australian index All Ordinaries (AORD) to 0.151 for the U.S. index Nasdaq (IXIC) index. Further enhancements to the approach we propose could involve making the analysis dynamic in order to assess both the stability of the roughness parameter over time and the presence of potential jumps in the volatility process. An indication that such a possibility exists is provided by the fact that, compared to the observations for the fOU process, in real data we detect a greater dispersion in the estimation of the self-similarity parameter as the time scale increases.

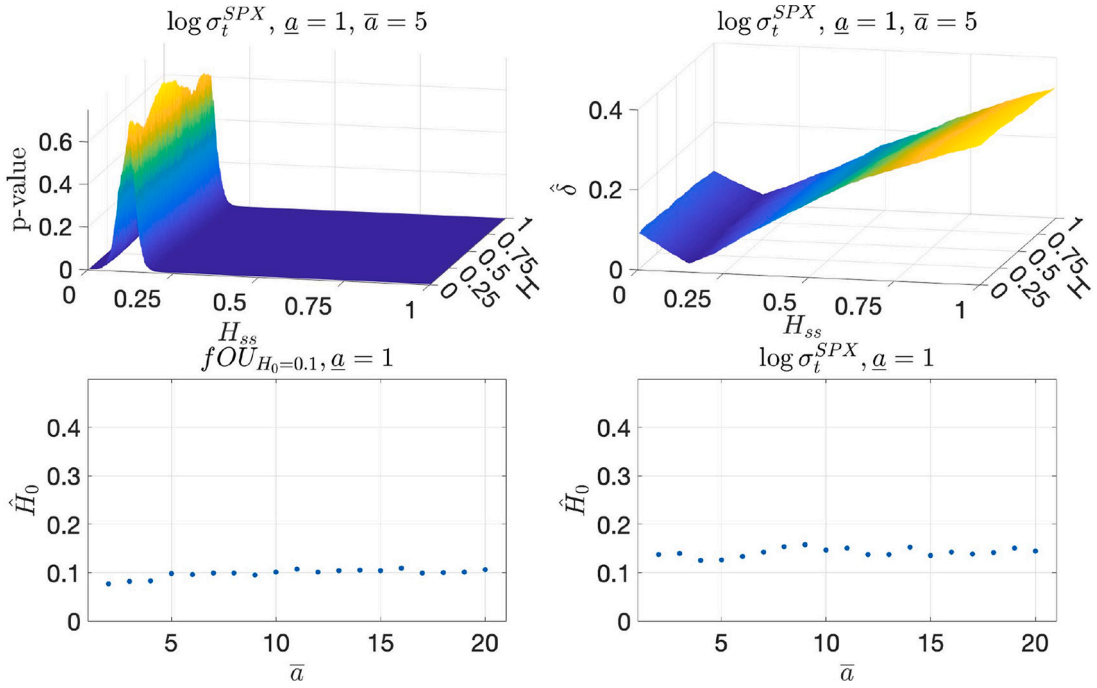

Fig. 5. Top panels: table displays the distances $\hat{\delta}$ and the p-values for the KS tests about increments of Lamperti transform of $\log \sigma_t$ for SPX index with a set of timescales $\mathcal{A} = [1, 5]$. Bottom left: the $\hat{H}_0$ values estimated for a fOU with $H_0 = 0.10$ for different $\overline{a} \in [\![2, 20]\!]$. $\hat{H}_0$ are dispersed around the prescribed H_0 with a mean of $\overline{\hat{H}_0} = 0.098 \pm 0.009$. Bottom right: the same analysis is displayed for the $\log \sigma_t$ of the SPX index with an estimated Hurst exponent $\overline{\hat{H}_0} = 0.142 \pm 0.009$.

CRediT authorship contribution statement

Sergio Bianchi: Conceptualization, Methodology, Writing, Supervision, Funding acquisition. **Daniele Angelini:** Conceptualization, Methodology, Software, Visualization, Writing. **Augusto Pianese:** Formal analysis, Investigation, Software, Visualization, Validation. **Massimiliano Frezza:** Formal analysis, Investigation, Data curation, Software, Resources.

Declaration of competing interest

The authors declare that they have no known competing financial interests or personal relationships that could have appeared to influence the work reported in this paper.

Data availability

Data will be made available on request.

Acknowledgments

The Authors would like to extend their appreciation to the Reviewers and Editor for investing their time and expertise in the comprehensive evaluation of the manuscript. The valuable comments and suggestions provided by them have been highly regarded and have contributed to the overall improvement of the manuscript's quality.

Funding

This research was supported by Sapienza University of Rome, Italy under Grant No. RM120172B346C021.

References

[1] Gatheral J, Jaisson T, Rosenbaum M. Volatility is rough. Quant Finance 2018;18(6):933–49.
[2] Bayer C, Friz P, Gatheral J. Pricing under rough volatility. Quant Finance 2016;16(6):887–904.
[3] El Euch O, Gatheral J, Rosenbaum M. Roughening heston. Risk 2019;84–9, Available at SSRN: https://ssrn.com/abstract=3116887.
[4] Livieri G, Mouti S, Pallavicini A, Rosenbaum M. Rough volatility: Evidence from option prices. IISE Trans 2018;50(9):767–76. http://dx.doi.org/10.1080/24725854.2018.1444297.
[5] Fukasawa M, Takabatake T, Westphal R. Consistent estimation for fractional stochastic volatility model under high-frequency asymptotics. Math Finance 2022;32(4):1086–132.
[6] Bolko E, Christensen K, Pakkanen M, Veliyeva B. A GMM approach to estimate the roughness of stochastic volatility. J Econometrics 2022. Available online 15 September 2022.
[7] Peng W, Muzy J-F, Bacry E. From rough to multifractal volatility: The log S-fBM model. Physica A 2022;604:127919.
[8] Bennedsen M, Lunde A, Pakkanen M. Decoupling the short- and long-term behavior of stochastic volatility. J Financ Econom 2021;20(5):961–1006. http://dx.doi.org/10.1093/jjfinec/nbaa049.
[9] Takaishi T. Rough volatility of Bitcoin. Finance Res Lett 2020;32:101379.
[10] Fukasawa M. Volatility has to be rough. Quant Finance 2021;21(1):1–8. http://dx.doi.org/10.1080/14697688.2020.1825781.
[11] Brandi G, Di Matteo T. Multiscaling and rough volatility: An empirical investigation. Int Rev Financ Anal 2022;84:102324.
[12] Cont R, Das P. Rough volatility: Fact or artefact? 2022, Available at SSRN: https://ssrn.com/abstract=4065951.
[13] Rogers L. Things we think we know. In: Lecture notes in finance options - 45 years since the publication of the Black-Scholes-Merton model. World Scientific; 2023, p. 173–84.
[14] Angelini D, Bianchi S. Nonlinear biases in the roughness of a Fractional Stochastic Regularity Model. Chaos Solitons Fractals 2023;172:113550.
[15] Bianchi S. A new distribution-based test of self-similarity. Fractals 2004;12(03):331–46. http://dx.doi.org/10.1142/S0218348X04002586.
[16] Lamperti J. Semi-stable stochastic process. Trans Amer Math Soc 1962;104:62–78.
[17] Embrechts P, Maejima M. Selfsimilar processes. Princeton University Press; 2002.
[18] Bianchi S, Pianese A, Frezza M. A distribution-based method to gauge market liquidity through scale invariance between investment horizons. Appl Stoch Models Bus Ind 2020;36:809–24.
[19] Doob J. The Brownian movement and stochastic equations. Ann of Math 1942;43(2):351–69.
[20] Durilleul P, Legendre P. Lack of robustness in two tests of normality against autocorrelation in sample data. J Stat Comput Simul 1992;42(1–2):79–91.
[21] Weiss M. Modification of the Kolmogorov-Smirnov statistic for use with correlated data. J Amer Statist Assoc 1978;73(364):872–5.
[22] Chicheportiche R, Bouchaud J-P. Goodness-of-fit tests with dependent observations. J Stat Mech: Theory Exp 2011;11:P09003.
[23] Lanzante J. Testing for differences between two distributions in the presence of serial correlation using the Kolmogorov–Smirnov and Kuiper's tests. Int J Climatol 2021;41(14):6314–23.
[24] Lim S, Muniandy S. Generalized Ornstein–Uhlenbeck processes and associated self-similar processes. J Phys A: Math Gen 2003;36:3961.
[25] Cheridito P, Kawaguchi H, Maejima M. Fractional Ornstein-Uhlenbeck processes. Electron J Probab 2003;8:1–14.
[26] Kaarakka T, Salminen P. On fractional Ornstein-Uhlenbeck processes. Commun Stoch Anal 2011;5(1):8.
[27] Kaarakka T. Fractional Ornstein-Uhlenbeck processes, publication 1338 (Ph.D. thesis), Tampere University of Technology; 2015.
[28] Garcin M. Hurst exponents and delampertized fractional Brownian motions. Int J Theor Appl Finance 2019;22(05):1950024.
[29] Wood AT, Chan G. Simulation of stationary Gaussian processes in [0, 1] d. J Comput Graph Statist 1994;3(4):409–32.